QUASIELASTIC VERSUS INELASTIC AND DEEP INELASTIC LEPTON SCATTERING IN NUCLEI AT $x > 1$

E. Marco and E. Oset.

Departamento de Física Teórica and IFIC, Centro Mixto Universidad de Valencia - CSIC, 46100 Burjassot (Valencia) Spain.

Abstract

We have made a thorough investigation of the nuclear structure function W_{2A} in the region of $0.8 < x < 1.5$ and $Q^2 < 20$ GeV^2, separating the quasielastic and inelastic plus deep inelastic contributions. The agreement with present experimental data is good giving support to the results for both channels. Predictions are made in yet unexplored regions of x and Q^2 to assert the weight of the quasielastic or inelastic channels. We find that at $Q^2 < 4$ GeV^2 the structure function is dominated by the quasielastic contributions for $x < 1.5$, while for values of $Q^2 > 15$ GeV^2 and the range of x studied the inelastic channels are over one order of magnitude bigger than the quasielastic one.

The potential of the structure function at $x > 1$ as a source of information on nuclear correlations is stressed once more.

1 Introduction

Deep inelastic scattering in nuclei has been a subject of intense study in the past years, which was stimulated by the discovery of the EMC effect [1]. Different reviews on the subject have incorporated the advances on the experimental and theoretical sides [2, 3, 4, 5, 6, 7]. With ups and downs several conventional effects have remained as important ingredients explaining the basic features of the experiment: pionic effects for the enhancement of the ratio of the F_2 nuclear structure function to the one of the deuteron [5, 8, 9, 10] around $x = 0.1$, binding effects for the depletion of that ratio around $x \simeq 0.6$ [11, 12, 13] and Fermi motion for the increase of the ratio for $x > 0.7$ [4, 8, 14].

Relativistic effects were also shown to be relevant [15, 16] and the use of spectral functions was advocated in refs. [17, 18] as an important tool to accurately account for Fermi motion and binding effects.

In a recent paper [19], a theoretical framework was developed which accounts very accurately for all these effects. It uses a relativistic formalism from the beginning and follows a Feynman diagrammatic many body scheme, where all the input from the nucleons or pions is incorporated via their respective propagators in the nuclear medium. The cloud from ρ-mesons was also found relevant in [19] and helped improve

the agreement with experiment. The scheme provided a good reproduction of the EMC data for different nuclei outside the shadowing region which was not explored.

On the other hand, interest has been growing in the region of $x > 1$. This region, inaccessible for free nucleons, clearly indicates nuclear effects and the Fermi motion is certainly the first candidate [13, 14, 20, 21]. In these latter works it was noted that a nonvanishing value of the nuclear structure functions at $x > 1 + k_F/M$ (with k_F the Fermi momentum) would indicate the presence of momentum components beyond the Fermi momentum and this is actually the case experimentally.

The high momentum components of the nucleus are generated by the nuclear correlations. For this reason the importance of these correlations in generating the structure function at large values of x has been emphasized repeatedly [2, 3, 22], although the relevant information on the spectral functions was not readily available at that time [3]. However, it is very dangerous to try to relate physical quantities to the occupation number, $n(\vec{k})$, since the high momentum components are strongly correlated with the energy of the nucleon and in physical processes one has conservation of fourmomentum. The importance of using the nucleon spectral function, $S_h(\omega, k)$, which provides the probability of finding a nucleon with a certain energy ω and a momentum k, was pointed out in refs. [17, 18, 23, 24, 25].

In ref. [26] a thorough study of the region of deep inelastic scattering for $x > 1$ was done for several nuclei. Several spectral functions were used. One of them [27] was calculated for infinite nuclear matter using a microscopic Brueckner-Hartree-Fock scheme and the NN interaction from realistic OBE potentials [28]. A second one was calculated semiphenomenologically [29], evaluating the nucleon selfenergy diagrams in a nuclear medium but using input from NN experimental cross sections and the polarization of the NN interaction in the medium to circumvent the use of the nucleon-nucleon potential and the ladder sums. In both cases the local density approximation was used to evaluate the structure functions for finite nuclei.

Another approach used a spectral function for finite nuclei [30] for the case of ^{16}O. An interesting result from ref. [26] is that the results with the local density approximation and those of the finite nuclei differ by less than 3% in the region of the EMC effect and at values of $x \simeq 1$ or bigger the differences are also less than 8%. The differences between the results with the two spectral functions of nuclear matter are of the same order of magnitude or smaller than those quoted above. This gives us confidence to rely upon the method in order to explore the $x > 1$ region where the information provided by the spectral function is essential. Indeed, it was found in ref. [26] that usual approximations, like the use of the non interacting Fermi sea, or the use of the momentum distribution $n(\vec{k})$ provided by the same spectral function, but taking $\omega = E(\vec{k})$ (the free nucleon energy), or even an average energy $\omega(\vec{k})$ weighted by the spectral function, gave rise to results which differed by two or three orders of magnitude from the accurate calculation and the experiment.

The realistic calculation using the spectral functions was compared with the only experiment at $x > 1$ in the deep inelastic region [31] and the results agree within $20 - 30\%$. The data of ref. [31] explore only the region of $x < 1.3$, and beyond 1.16 the data are only upper bounds. It was also found in ref. [26] that the region of $x \approx 1.3-1.4$

was only sensitive to the high momentum and binding components provided by the nuclear correlations and that the shell model part of the nuclear spectral function gave a negligible contribution in that region.

It is thus clear that more data in the $x > 1$ region are necessary to further study these interesting dynamical properties of nuclei beyond the simple shell model picture [32]. This is the same conclusion raised in ref. [7], which states that high Q^2 data at high x should be a top priority.

On the other hand, many more data at lower values of Q^2 exist, mostly measured at SLAC [33, 34], which could shed light on the same nuclear issues, and others are planned at TJNAF [35]. However, it was soon noticed that these data have a large contamination of quasielastic contribution where one nucleon of the nucleus is knocked out but there is no particle production from this individual nucleon [24, 36, 37, 38]. The presence of this quasielastic background helped interpret the "accidental" ξ scaling observed in these reactions [39].

In ref. [37] three different regions are differentiated: the quasielastic, the inelastic and the deep inelastic regions. The first one corresponds to one nucleon removal, the second one to the excitation of low lying resonances which decay by pion emission and the third one to deep inelastic where more particles are produced. As quoted in ref. [37] these three regions are never completely separated although one can find the dominance of some of these channels in different regions. The investigations of ref. [37] concluded that the region of $x > 1$ and $Q^2 < 3$ GeV^2 is dominated by the quasielastic process and that $Q^2 > 20$ GeV^2 is a safe region where the deep inelastic process would dominate at $1 < x < 2$.

The work of refs. [19, 26] improves over the method used in refs. [17, 18] in the use of a relativistic framework which makes unnecessary the flux factor proposed in ref. [40] and used in refs. [17, 18] in order to introduce relativistic effects in the nonrelativistic calculations. It was shown in ref. [19] that the latter procedure led to different numerical results than the consistent relativistic calculation. In addition, the work of ref. [19] included the contribution from the modification of the meson cloud in the medium, however, this feature is irrelevant in the $x > 1$ region since the mesonic effects become negligible beyond $x > 0.6$.

With the advent of future experiments at intermediate energy machines like TJNAF, or possible ones in proposed facilities like ELFE, it becomes important to make an exploration of that region in order to assess the dominance of the different processes at different Q^2 and x and the characteristics of the different processes. This is the aim of the present paper which complements the findings of ref. [37].

2 Formalism for inelastic lepton scattering

We follow closely the formalism of ref. [19] and write the inelastic lepton nucleus cross section as

$$\frac{d^2\sigma}{d\Omega dE'} = \frac{\alpha^2}{q^4} \frac{k'}{k} L'_{\mu\nu} W'^{\mu\nu}_A \qquad (1)$$

where k, k' are the momenta of the incoming and outgoing lepton and q the virtual photon momentum (see fig. 1). In eq. (1), $L'_{\mu\nu}$ is the lepton tensor

$$L'_{\mu\nu} = 2k_\mu k'_\nu + 2k'_\mu k_\nu + q^2 g_{\mu\nu} \tag{2}$$

and $W_A'^{\mu\nu}$ is the hadronic tensor. We can use eq. (39) of ref. [19] by means of which the nuclear hadronic tensor, in the local density approximation, can be written in terms of the nucleon one as

$$W_A'^{\mu\nu} = 4 \int d^3r \int \frac{d^3p}{(2\pi)^3} \frac{M}{E(\vec{p})} \int_{-\infty}^\mu dp^0 S_h(p^0, p) W_N'^{\mu\nu}(p, q)$$

with

$$p \equiv (p^0, \vec{p}); \quad W_N'^{\mu\nu} = \frac{1}{2}(W_p'^{\mu\nu} + W_n'^{\mu\nu}) \tag{3}$$

By following the prescription of ref. [19], $W_N'^{\mu\nu}(p, q)$, which appears with nucleon variables off shell, is evaluated by taking the matrix elements on shell $(E(\vec{p}), \vec{p})$, while the δ functions of conservation of fourmomentum are strictly kept with the off shell variables. In eq. (3) $S_h(p^0, p)$ is the spectral function for hole states of the correlated Fermi sea, normalized as

$$4 \int d^3r \int \frac{d^3p}{(2\pi)^3} \int_{-\infty}^\mu S_h(\omega, p, k_F(\vec{r})) d\omega = A \tag{4}$$

in symmetric nuclear matter, where μ is the chemical potential.

Gauge invariance imposes the following structure of the hadronic tensor in terms of two invariant structure functions W_1, W_2,

$$W'^{\mu\nu} = \left(\frac{q^\mu q^\nu}{q^2} - g^{\mu\nu}\right) W_1 + \left(p^\mu - \frac{p \cdot q}{q^2} q^\mu\right)\left(p^\nu - \frac{p \cdot q}{q^2} q^\nu\right) \frac{W_2}{M^2} \tag{5}$$

Furthermore, in the Bjorken limit W_1 and W_2 are related by the Callan-Gross relation and hence all information is given by one of the structure functions and W_2 is usually chosen for presentation of the data. In the studies of inelastic scattering at lower values of Q^2 it is also customary to show results for W_2, hence we use eqs. (3) and (5) to write W_{2A} in terms of W_{2N} by eliminating the structure function W_1. This is easily accomplished by using the expressions for W'^{xx} and W'^{zz} and taking q in the z direction, as usually done, and we get

$$W_{2A} = -\frac{q^2}{|\vec{q}|^2} \sum_{p,n} 2 \int d^3r \int \frac{d^3p}{(2\pi)^3} \frac{M}{E(\vec{p})} \int_{-\infty}^\mu d\omega \, S_h(\omega, |\vec{p}|)$$

$$\times \, [(p^x)^2 - \frac{q^2}{q^{02}} (p^z - \frac{p.q}{q^2}|\vec{q}|)^2] \frac{W_{2N}(p, q)}{M^2} \tag{6}$$

where we have substituted a factor 2 of isospin in eq. (3) by the explicit sum over protons and neutrons (see also ref. [42] for these Fermi motion corrections).

In the Bjorken limit, when $-q^2 \to \infty, q^0 \to \infty$, we define the variables

4

$$x_N = \frac{-q^2}{2pq}; \ \nu_N = \frac{p \cdot q}{M}; \ Q^2 = -q^2; \ x = \frac{-q^2}{2Mq^0}; \ \nu = q^0 \tag{7}$$

and the structure functions

$$\nu_N W_2(x_N, Q^2) \equiv F_2(x_N, Q^2)$$
$$MW_1(x_N, Q^2) \equiv F_1(x_N, Q^2) \tag{8}$$

where F_1, F_2 depend only on x_N (there are smooth QCD corrections depending on Q^2) and we find

$$F_{2A}(x) = \sum_{p,n} 2 \int d^3r \int \frac{d^3p}{(2\pi)^3} \frac{M}{E(\vec{p})} \int_{-\infty}^{\mu} d\omega S_h(\omega, |\vec{p}|) \frac{x}{x_N} F_{2N}(x_N) \tag{9}$$

which is the expression found in ref. [19] for the F_{2A} structure function in the Bjorken limit.

Eq. (6) allows us to take into account the small corrections from the terms with p^x and p^z in the bracket of the formula, which become negligible in the Bjorken limit. We use this equation to evaluate the inelastic plus deep inelastic part of the nuclear structure function.

In the case of the quasielastic contribution to the structure function, W_{2A}^Q, we evaluate it explicitly from the imaginary part of the lepton selfenergy of the diagram of fig. 2. By following the steps of section 3 of ref. [19] we can write:

$$W'^{\mu\nu} = \sum_{n,p} 2 \int d^3r \int \frac{d^3p}{(2\pi)^3} \frac{M}{E(\vec{p})} \int_{-\infty}^{\mu} S_h(p^0, p) dp^0$$
$$\frac{M}{E(\vec{p}+\vec{q})} \bar{\sum}_{s_i} \sum_{s_f} \langle p + q|J^\mu|p\rangle \langle p + q|J^\nu|p\rangle^* \delta(q^0 + p^0 - E(\vec{p} + \vec{q})) \tag{10}$$

where J^μ is the ordinary current for the coupling of a photon to a nucleon [43].

As advocated in ref. [19], we follow here the philosophy of taking the matrix elements of the current between free spinors (dependent on threemomentum only) while keeping the argument of the δ function with the variables strictly off shell as they are provided by the nuclear spectral function.

In terms of the Sachs form factors G_E, G_M we can write the matrix elements of eq. (10) as:

$$\bar{\sum}_{s_i} \sum_{s_f} \langle p + q|J^\mu|p\rangle \langle p + q|J^\nu|p\rangle^* =$$
$$= \left\{ \frac{p_x^2}{M^2}(1 - \frac{q^2}{4M^2})^{-1}[G_E^2(q) - \frac{q^2}{4M^2}G_M^2(q)] - \frac{q^2}{4M^2}G_M^2(q) \right\} \quad \text{for } \mu, \nu = x, x$$
$$= \left\{ \frac{1}{4M^2}(1 - \frac{q^2}{4M^2})^{-1}[G_E^2(q) - \frac{q^2}{4M^2}G_M^2(q)](2E(p) + q^0)^2 - \frac{\vec{q}^2}{4M^2}G_M^2(q) \right\} \quad \text{for } \mu, \nu = 0, 0 \tag{11}$$

W_{2A}^Q is given by means of eq. (5) for the nucleus at rest by

$$W_{2A}^Q = (\frac{q^2}{\vec{q}^2})^2 W_{A,Q}'^{00} - \frac{q^2}{\vec{q}^2} W_{A,Q}'^{xx} \tag{12}$$

5

Hence, by means of eqs. (10), (13), (14) we can evaluate the quasielastic structure function W_{2A}^Q.

For the W_{2N} inelastic plus deep inelastic structure function of the nucleon we take the parametrization of refs. [14, 41] where there is a part corresponding to the excitation of low lying resonances (usually called the inelastic part) and a smooth part for excitation in the continuum which would stand for the deep inelastic part.

For the electric and magnetic form factors we take the dipole parametrization of ref. [44]

3   Results and discussion

In figs. 3, 4, 5 we show the results for the structure function W_{2A} (νW_{2A} in the figures) for ^{56}Fe. The figures show the strength of the structure function as a function of x, but Q^2 is related to x in the experiment since the data correspond to the scattering of electrons with a fixed initial energy, a fixed angle for the final electron and variable energy for the final electron. In fig. 3 the initial energy is $E = 3.595\,GeV$ and angle $\theta = 20^0$ [33]. In this case at $x = 1$ one has $Q^2 = 1.27$ GeV^2 and Q^2 increases as x increases. In fig. 4 $E = 3.595\,GeV$, $\theta = 39^0$ [33], and $Q^2 = 3.1$ GeV^2 at $x = 1$. In fig. 5 $E = 5.12$ GeV, $\theta = 56.6^0$ [34] and $Q^2 = 6.83$ GeV^2 at $x = 1$. The nucleon structure function has been taken from ref. [41].

In fig. 3 we can see the results for the quasielastic and inelastic contributions. The quasielastic contribution is dominant in all the range of the figure and peaks around $x = 1$ (for on shell nucleons at rest we would have a $\delta(x-1)$ function). The spread of the quasielastic contribution is due to Fermi motion and binding. The inelastic plus deep inelastic contribution is small (we will call it inelastic for simplicity in what follows) in all the range of the figure compared to the quasielastic contribution. However, at values of $x < 1$ the inelastic contribution becomes more relevant. In fact one can see in the figure that at $x = 0.8$ the inelastic contribution is about 70 % of the quasielastic one, and its inclusion is necessary to obtain a good agreement with the data in that region. For values of $x > 1$ the strength of the structure function is completely dominated by the quasielastic contribution. The agreement with experiment is rather good up to values of $x = 1.4$ and from there on our results start diverging from the data.

The region of $x > 1.5$ in the figure can be filled up by excitation of $2p2h$ components, either by renormalizing the final nucleon propagator (we have taken a free propagator for the ejected nucleon) or incorporating meson exchange currents (MEC) into the approach. It is easy to see that the $2p2h$ excitation is favoured in the $x > 1.5$ with respect to the $1p1h$ excitation. Indeed, by splitting the fourmomentum $q^0, \vec{q}$ into two equal halves with $q^0/2, \vec{q}/2$ for each ph excitation as an average, we see that this latter combination is kinematically much more suited than the excitation of a ph component with $q^0, \vec{q}$.

The contribution of these $2p2h$ components has been the subject of intense investigation at lower electron energies [45, 46, 47, 48]. It is a genuine many body contribution which is not accounted for by the inelastic contribution and hence is additional to the quasielastic and inelastic channels studied here (the final nucleon renormalization ac-

tually redistributes the strength and is not an additive channel, contrary to the case of the MEC).

We will not discuss further this subject since our purpose here is to make a comparison of the quasielastic with the inelastic contribution as a function of Q^2 and x to establish the regions where the inelastic contributions dominate in the cross sections.

In fig. 4 we find similar features to those discussed above except that we see that the contribution of the inelastic channels is relatively more important than in the former case. Indeed, at $x = 0.95$ the quasielastic and inelastic contributions are about the same. Once again we can see that the inelastic contribution is essential to describe quantitatively the data below $x = 1$ and at $x < 0.9$ the inelastic contribution dominates the structure function.

In fig. 5 we show the results for the recent experimental data of ref. [34] taken at higher electron energies and Q^2. At this value of Q^2 we see that the quasielastic and inelastic contributions are similar around $x = 1.2$ but at higher and lower values of x the inelastic contribution is larger, particularly at $x \leq 1$ where it becomes clearly dominant.

We can see from all these figures that the agreement of our results with the data in the regions of dominance of the inelastic or quasielastic channels is rather good and we then extrapolate the results to make predictions for values of Q^2 still unexplored.

One interesting finding of ref. [26] is the sensitivity to the nuclear spectral function $S_h(\omega, p)$ of the results for the structure functions F_{2A} at $x > 1$ and Q^2 large, and how some common approximations made in the study of the EMC effect badly fail at values of $x = 1.2 - 1.5$. Here we want to carry out a similar test for the quasielastic channel and for the inelastic one at these lower values of Q^2.

In fig. 6 we show the results of the quasielastic channel calculated with the spectral function and with two approximations:

1) Non interacting Fermi sea, for which the spectral function can be written as [26]

$$S_h^{FS}(\omega, p, \rho) = n_{FS}(\vec{p})\delta(\omega - E(\vec{p}) - \Sigma) \tag{13}$$

where n_{FS} is the occupation number of a non interacting Fermi sea of local density $\rho(r)$.

The magnitude Σ in eq. (13) is a selfenergy which is chosen such as to provide the exact experimental binding energy of each particular nucleus [26].

2) Momentum distribution. In this case we use eq. (13), with a momentum distribution $n_I(\vec{p})$ which is the actual momentum distribution in the nucleus given by

$$n_I(\vec{p}) = \int_{-\infty}^{\mu} S_h(\omega, p)d\omega \tag{14}$$

This approximation misses the correlations of the momenta with the energy and we shall call it uncorrelated momentum distribution.

In fig. 6 we see that the use of the non interacting Fermi distribution leads to similar results (slightly bigger) of the structure function around the peak of the distribution (at $x = 1$) than those using the spectral function. However, as x increases, the results with the non interacting Fermi sea fall faster than the other ones.

The spectral function accounts for larger momentum components than the non interacting Fermi sea and this is the reason for the extended contributions at $x > 1$. We also show in the figure the results obtained by using the uncorrelated momentum distribution of eq. (14). We can see that this approximation fails to provide the main features of the quasielastic peak, which are well given by the non interacting Fermi sea calculation or the one using the spectral function. We also observe that at $x > 1.6$ the approximation gives rise to an important contribution which is not substantiated by the accurate calculation with the spectral function. This is due to the contribution of large momentum components which, however, are uncorrelated with similarly large binding energies, as the spectral function would give [26].

In fig. 7 we see similar results but for the inelastic contribution corresponding to the data of fig. 5. In this case the roles are reversed. We can see that the non interacting Fermi sea gives results smaller than those with the spectral function at $x > 1$ and the uncorrelated momentum distribution gives rise to results much bigger than those obtained with the spectral function at $x > 1$. The discrepancies are rather large, such that none of these approximations can be advocated as a fair substitute of the use of the full spectral function. Particularly, the results obtained with the momentum distribution are rather bad in both channels, the quasielastic and the inelastic.

Another way of expressing these ideas is to say that the inelastic contribution at $x > 1$ is rather sensitive to the nuclear spectral function and carries information on this magnitude, particularly, as discussed in ref. [19], about the "background" contribution which is tied to the dynamical features of the nucleus.

Now we proceed to extrapolate the results at higher Q^2. In fig. 8 we show the results for the quasielastic and inelastic contributions at $x = 1$ as a function of Q^2. We use three different parametrizations of the nucleon structure function, one of them which we have used so far [41], and which is indicated for relatively low Q^2 and other two, [49] (MRS) and [50] (CTEQ), which are more suited for large Q^2 values in the Bjorken scaling region. The figure is significative because we see that the results obtained for the inelastic contribution are very sensitive to the parametrization used for the nucleon structure function. At $Q^2 = 20 \ \mathrm{GeV}^2$ the results obtained with different nucleon structure functions differ by about a factor 5. However, at values of $Q^2 \simeq 1$ GeV^2 the differences are about a factor 50. A discussion of the assumptions made in these structure functions and their range of validity is hence in order. The structure function from CTEQ which we use is meant to be used at large Q^2 in the Bjorken scaling region, since we do not implement Q^2 corrections important at small Q^2. The structure function of MRS is meant to work at high values of Q^2 and also at low values and hence, in principle, should cover the range of Q^2 in fig. 8. However, data at small Q^2 and large x are not included in the fit of MRS. Indeed, the largest x considered is $x = 0.85$ and the data for this value of x go down to $Q^2 = 10 \ \mathrm{GeV}^2$ only.

On the other hand, the parametrization of ref. [41] is precisely meant for low values of Q^2 and it contains the contribution from excitation of resonances (the so called inelastic part) plus a background of deep inelastic. This parametrization is done with precission, observing also the thresholds. For instance $F_{2N}(x)$ vanishes before $x = 1$ as it should be: Indeed, we have

$$s = Q^2(\frac{1}{x} - 1) + M^2 > (M + m_\pi)^2 \qquad (15)$$

since we need to create at least a pion in the inelastic contribution. Hence, in the limit $Q^2 \to \infty$, we have $0 < x < 1$ and the limit of $x = 1$ can be approached as much as one wishes. However, for Q^2 of the order of a few GeV^2 there is a cut off at values of $x < 1$, for example at $Q^2 = 1$ GeV^2 , we have $x < 0.78$. The parametrization of [41] has a structure function vanishing in the forbidden region, while the one of MRS provides a smooth function of x which reaches the limit $x = 1$ for all values of Q^2.

Since the nuclear structure function F_{2A} calculated at $x > 1$ picks up its contribution from F_{2N} for values of x_N close to 1, it is then clear that the structure function of MRS should not be used for such purposes for low values of Q^2. Instead, the nucleon structure function of [41] should be used in this case. But the latter one should not be used at large values of Q^2.

A compromise region can be $Q^2 \simeq 6 - 7$ GeV^2 below which the [41] results should be taken and beyond which the MRS should be used. The problems with the MRS and CTEQ parametrizations to describe the large x region can be further exposed in figs. 9, 10, 11.

In fig. 9 we show the results for F_{2A} at $x = 0.8$ with the three parametrizations. We see now a better agreement between the MRS and [41] parametrizations in the region of 3 GeV$^2 \le Q^2 \le 8$ GeV^2. Below $Q^2 = 3$ GeV^2 we see again that the MRS gives a sharp increase with respect to [44] which again must be attributed to the artificial large x dependence of F_{2N}. At values of $Q^2 > 15$ GeV^2 the CTEQ and MRS parametrizations start converging.

The discrepancies between the results of F_{2A}, calculated with the different nucleon structure functions at $x = 1$ in fig. 8, become even worse at higher values of x. In fig. 10 we show the results at $x = 1.3$. Discarding the results obtained with the CTEQ parametrization in that region, we still see that there are large discrepancies between the MRS and [41] results with a gap in the region of $Q^2 \simeq 6$–7 GeV^2 which should in principle be the dividing region for the two results. It is difficult to draw firm conclusions in the region of 4 GeV$^2 < Q^2 < 15$ GeV^2, but we can safely claim that at values of $Q^2 < 4$ GeV^2 the quasielastic contribution dominates the nuclear structure function, while at $Q^2 > 15$ GeV^2 the inelastic part dominates.

The situation becomes even worse at $x = 1.5$ (not shown here). Once again it is difficult to make up one's mind in the intermediate region of Q^2, but in any case one could conclude rather safely the dominance of the inelastic channel at $Q^2 > 20$ GeV^2 and of the quasielastic one at $Q^2 < 3$ GeV^2. These results agree with those obtained in ref. [37].

It is clear that going to values of $x > 1.5$ would make the results even more sensitive to the parametrization of F_{2N}, thus increasing more the intrinsic uncertainties of the nuclear structure function and not allowing the extraction of useful nuclear information.

There is, however, good news if one goes to high values of Q^2 in the Bjorken region. Indeed, as we show in fig. 11, at $Q^2 \simeq 85$ GeV^2 the nuclear structure function F_{2A} is all due to the inelastic contributions and the results obtained with different parametrizations agree remarkably among themselves, which gives us great confidence

9

in the results. We have carried out the calculations using three parametrizations: the MRS, the one of CTEQ and the one of Duke and Owens [51]. The differences are of the order of 10% or less. We also show in the figure the experimental results of ref. [31] The results agree with the data within 30% in the range of $0.8 < x < 1.3$. As discussed in ref. [26] the results of F_{2A} at $x > 1$ are essentially due to the "background" part of the nuclear spectral function, with a negligible contribution of the bound states of the shell model. The structure function hence contains a very rich information on "nuclear correlations" in the generalized sense of nuclear structure beyond the mean field approximation.

Coming back to our discussion about the accuracy of the different nucleon structure functions to provide F_{2A} at $x > 1$ we show in fig. 12 the results obtained for $Q^2 = 1.27$ GeV^2 (at $x = 1$) with the MRS structure function. We can see that the addition of the inelastic contribution to the quasielastic one leads to poor agreement with the data. This confirms our previous statements that at low Q^2 the MRS should give an overestimate of F_{2A} because it does not respect the thesholds in x.

On the other hand, in fig. 13 we show the results calculated with the MRS structure function at $Q^2 = 6.83$ GeV^2 (at $x = 1$). The agreement with the data in this case is of the same quality as with the Stein structure function [41], slightly better at high values of x and slightly worse at smaller x. This figure substantiates our statement that $Q^2 \simeq 6 - 7$ GeV^2 is the dividing line for the validity of the two parametrizations and values of x around 1 or below. At larger values of x we saw, however, that in that region there are discrepancies between the results with the two structure functions.

Another message of our results is that if one wants to extract useful nuclear information at values of $x > 1.3$ from the intermediate Q^2 region (3 GeV$^2 < Q^2 < 15$ GeV^2), a reliable nucleon structure function in the region of x close to 1 is absolutely necessary. This call is important in view that this range is bound to be covered in future experiments at TJNAF.

It is interesting to compare these results with those found in ref. [37]. The results found here at $x = 1$ are very similar to those found in ref. [37], qualitatively and quantitatively. At values of $x > 1$ the trend of our results agree qualitatively with those of ref. [38]. However, our discussion and the use of different nucleon structure functions served to show that at present there are large uncertainties in the intermediate Q^2 region tied to the behaviour of the structure functions at x close to 1, which prevent us from drawing firm conclusions in that region.

4   Conclusions

We have made a thorough study of the quasielastic and inelastic contributions to the nuclear structure functions in the region of $x \geq 1$ and for values of Q^2 ranging from 1-20 GeV^2. This is the region where both mechanisms compete and we have shown the regions in the x, Q^2 variables where one or the other of the mechanisms dominates. As discussed in the former section, in some cases we reconfirm results obtained by other authors before, but there are a few novelties in the present work. With respect to ref. [26], where only deep inelastic scattering at high Q^2 was studied, we study here the

region of small and intermediate Q^2 and include the quasielastic contribution which was negligible at high Q^2. This has allowed us to compare our theoretical predictions with many existing data, which had not been done before, and also has allowed us to make some prospects of what can be learned and what should then be measured in present facilities like TJNAF.

With respect to the similar work of refs. [37, 38] our results include relativistic corrections. Furthermore, our study has shown that there is no precise information available on the nucleon structure functions around $x = 1$ in order to make reliable predictions in the region of 6 GeV$^2 < Q^2 < 20$ GeV^2. We also give arguments which set clear limits to the region of validity of present parametrizations of the nucleon structure functions. On the other hand, even if we have different numerical results at $x > 1$ than in [37, 38], the "safe" conclusions obtained here (taking into account the uncertainties) about the regions of dominance of the quasielastic or deep inelastic contributions are the same. We describe now with some more details the main findings of the present work.

On general grounds we can say that at $x = 1$ the quasielastic contribution dominates below $Q^2 < 3$ GeV^2 while for $Q^2 > 13$ GeV^2 the inelastic contribution is already an order of magnitude bigger than the quasielastic one.

For values of $x > 1.3$ we found that in the region of 3 GeV$^2 < Q^2 < 15$ GeV^2 the results for the inelastic contribution obtained with different nucleon structure functions were very different. This does not allow one to draw strong conclusions from the data in that region.

We also observed that at values of $Q^2 \simeq 85$ GeV^2 the results obtained for F_{2A} at $x > 1$ with different nucleon structure functions were very stable. This fact, together with the sensitivity of these results to the region of large momenta and binding energies of the nuclear spectral function, makes the measurement of F_{2A} in that region an excellent tool to learn about dynamical aspects of the nucleus, beyond its approximate shell model structure.

Even with the uncertainties about the inelastic contribution in the intermediate Q^2 region, we can make some relatively safe statements by claiming that for $x < 1.5$ the inelastic contribution is dominant for $Q^2 > 20$ GeV^2 while the quasielastic contribution is dominant for $Q^2 < 4$ GeV^2. These results confirm the findings of ref. [37].

Our determination of the quasielastic contribution is rather precise in the region of $Q^2 < 20$ GeV^2. This means that if experiments are done in that region, our results can be used to separate the inelastic contribution to the structure function from the data. These results would be useful to unravel the discrepancies between different models for F_{2N} at x close to 1. Certainly, precise measurements of F_{2N} in that region would also be needed simultaneously if one wishes to asses the validity of the many body methods used here. Taking into account that this range of Q^2 is the one likely to be investigated at TJNAF, both types of experiments are called for.

With respect to the reliability of the method used, there are two regions where our predictions for the inelastic contribution are safe: the region of $Q^2 < 5$ GeV^2 where the parametrization for F_{2N} of [41] used here is rather reliable, and the one in the deep inelastic region at $Q^2 > 80$ GeV^2 where the results obtained are rather stable, quite independent of the parametrization used.

At large Q^2 the agreement of our results with the only existing data is fair. At low values of Q^2 the agreement of our results with the data is rather good and by changing the range of Q^2 and x we change the strength of the inelastic and quasielastic contributions, obtaining in all cases a good agreement with the data (at $x < 1.5$, $Q^2 < 5$ GeV^2). This gives us some confidence in our method to describe both the quasielastic and inelastic contributions in those regions.

Another interesting information which one could get experimentally is the separation between the quasielastic contribution and the inelastic one. Here, however, we must give an anticipated warning about how the comparison should be made. In the evaluation of the quasielastic contribution we did not look at final state interaction (FSI). This is fine is one wishes to obtain the contribution from this channel to the F_{2A} structure function, which sums the contributions of all possible final states. In practice, the strength of the quasielastic channel evaluated by us would be redistributed in other channels due to final state interaction of the emerging nucleon with the nucleus, and hence some events which were quasielastic originally will become inelastic ones in the nucleus due to FSI. This is in complete analogy with the process of photon absortion in nuclei, which can proceed either through direct photon absorption by pairs (or trios) of nucleons or indirectly via pion production and pion reabsorption in the nucleus [52]. In this case, events which were pion production originally become nuclear absorption events, but the important thing is that the inclusive cross section can be calculated by looking only at the first step processes. The FSI does not change the cross sections obtained in that way, it simply redistributes the strength in other channels. Certainly, one of the possible measurements would be one nucleon emission and the rest of the nucleus in its ground state. This is not a trivial measurement since it requires a good energy resolution to guarantee that the final nucleus is not further excited. Provided this experiment is done, the comparison of our results with this data would require the use of distorted waves for the emitted nucleon, instead of the implicit plane wave calculation which we have done. On the other hand, if what one wishes is to separate the inelastic contribution to be compared with ordinary evaluations of the deep inelastic nuclear structure function, what one must subtract from the data is not this experimental one (and only one) nucleon removal contribution, but the quasielastic scattering contribution evaluated by us, corresponding to the first step quasielastic scattering on one nucleon.

Summarizing our thoughts on future perspectives: the measurements at $x > 1$ in the high Q^2 region, $Q^2 \simeq 80$ GeV^2 should be encouraged. They offer a clean measure of the deep inelastic contribution and they provide direct information on the dynamical aspects of the nucleus, loosely speaking, about nuclear correlations. Certainly other theoretical calculations should be most welcome.

The region of low Q^2, $Q^2 < 5$ GeV^2 and $x \leq 1$ seems to be rather well under control theoretically but there the quasielastic contribution is large. The quasielastic contribution at low values of Q^2 is only sensitive to nuclear correlations for $x > 1.5$ where other contributions would be important, hence it can not be considered an important source of information on the dynamical aspects of the nucleus. Conversely, the inelastic and deep inelastic contributions, even at intermediate values of Q^2 carry this relevant information. The existence of experimental facilities where this region

12

of Q^2 will be explored can rend this information easily accessible. However, for the purpose of capitalizing the information contained in these data, the measurement of nuclear structure functions at $x > 1$ in that region should be accompanied by precise measurements and accurate parametrizations of the nucleon structure function at x close to 1.

References

[1] J.J. Aubert et al., Phys. Lett. B 123 (1983) 275.

[2] L.L. Frankfurt and M.I. Strikman, Phys. Rep. 76 (1981) 215.

[3] L.L. Frankfurt and M.I. Strikman, Phys. Rep. 160 (1988) 236.

[4] R.P. Bickerstaff and A.W. Thomas, J. Phys. G 15 (1989) 1523.

[5] A.B. Migdal, E.E. Saperstein, M.A. Troitskii and D.N. Voskresenskii, Phys. Rep. 192 (1990) 179.

[6] M. Arneodo, Phys. Rep. 240 (1994) 301.

[7] D.F. Geesaman, K. Saito and A.W. Thomas, Annu. Rev. Nucl. Part. Sci. 45 (1995) 337.

[8] C.H. Llewellyn Smith, Phys. Lett. B128 (1983) 107.

[9] M. Ericson and A.W. Thomas, Phys. Lett. B128 (1983) 112.

[10] V. Sanjosé, V. Vento and S. Noguera, Nucl. Phys. A 470 (1987) 509; P. González and V. Vento, Mod. Phys. Lett. A 8 (1993) 1563.

[11] S.V. Akulinichev, S.A. Kulagin and G.M. Vagradov, Pis'ma Zh. Eksp. Teor. Fiz. 42 (1985) 105; JEPT Lett. 42 (1985) 127; Phys. Lett. B 158 (1985) 485.

[12] G.V. Dunne and A.W. Thomas, Phys. Rev. D 33 (1986) 2061.

[13] S.V. Akulinichev and S. Shlomo, Phys. Rev. C 33 (1986) 1551.

[14] A. Bodek and J.L. Ritchie, Phys. Rev. D 23 (1981) 1070.

[15] F. Gross and S. Liuti, Phys. Rev. C 45 (1992) 1374.

[16] S. Liuti and F. Cross, Phys. Lett. B 356 (1995) 157.

[17] C. Ciofi degli Atti and S. Liuti, Phys. Lett. B 225 (1989) 215.

[18] C. Ciofi degli Atti and S. Liuti, Phys. Rev. C 44 (1991) R 1269.

[19] E. Marco, E. Oset and P. Fernández de Córdoba, Nucl. Phys. A 611 (1996) 484.

[20] H. Araseki and T. Fujita, Nucl. Phys. A 439 (1985) 681.

[21] K. Saito and T. Uchiyama, Z. Phys. A 322 (1985) 299.

[22] M. Ericson, Abstracts of the PANIC Kyoto Conference 1987, Eds. S. Homma, M. Morita, K. Nakai and T. Yamazaki, North Holland, pag. 416c.

[23] C. Ciofi degli Atti and S. Liuti, Phys. Rev. C 41 (1990) 1100.

[24] S. Liuti, Phys. Rev. C 47 (1993) R 1854.

[25] S. Simula, Few Body Systems Suppl. 8 (1995) 423.

[26] P. Fernández de Córdoba, E. Marco, H. Müther, E. Oset and A. Faessler, Nucl. Phys. A 611 (1996) 514.

[27] H. Müther, G. Knehr and A. Polls, Phys. Rev. C 52 (1995) 2955.

[28] R. Machleidt, Adv. Nucl. Phys. 19 (1989) 189.

[29] P. Fernández de Córdoba and E. Oset, Phys. Rev. C 46 (1992) 1697.

[30] H. Müther, A. Polls and W.H. Dickhoff, Phys. Rev. C 51 (1995) 3040.

[31] A.C. Benvenuti et al., Z. Phys. C 63 (1994) 29.

[32] C. Mahaux, P.F. Bortignon, R.A. Broglia and C.H. Dasso, Phys. Rep. 120 (1985)1.

[33] B.W. Filippone et al., Phys. Rev. C 45 (1992) 1582.

[34] J. Arrington et al., Phys. Rev. C 53 (1996) 2248.

[35] D.B. Day, private communication.

[36] L.L. Frankfurt, M.I. Strikman, D.B. Day and M. Sargsyan, Phys. Rev. C 48 (1993) 2451.

[37] C. Ciofi degli Atti., D.B. Day and S. Liuti, Phys. Rev. C 46 (1992) 1045.

[38] C. Ciofi degli Atti and S. Simula, Phys. Lett. B 325 (1994) 276.

[39] O. Benhar and S. Liuti, Phys. Lett. B 358 (1995) 173.

[40] L.L. Frankfurt and M.I. Strikman, Phys. Lett. B 183 (1987) 254.

[41] S. Stein et al., Phys. Rev. D 12 (1975) 1884.

[42] P.J. Mulders, Phys. Rep. 185 (1990) 83.

[43] C. Itzykson and J.B. Zuber, Quantum Field Theory (McGraw-Hill, New York,1980).

[44] E. Amaldi, S. Fubini and G. Furlan, Pion Electroproduction, Springer tracts in modern Physics, 83 (1979), Springer, Berlin.

[45] W. Alberico, M. Ericson and A. Molinari, Ann. Phys. 154 (1984) 356.

[46] W.M. Alberico, A. Molinari, R. Cenni and P. Saracco, Ann. Phys. 174 (1987) 131.

[47] M.J. Dekker, P.J. Brussard and T. Tjon, Phys. Lett. B 289 (1992) 255.

[48] A. Gil, PhD Thesis, University of Valencia, A. Gil, J. Nieves and E. Oset, preprint.

[49] A.D. Martin, W.J. Stirling and R.G. Roberts, Phys. Rev. D 51 (1995) 4756.

[50] H.L. Lai et al., Phys. Rev. D 51 (1995) 4763.

[51] D.W. Duke and J.F. Owens, Phys. Rev. D 30 (1984) 49.

[52] R.C. Carrasco, E. Oset and L.L. Salcedo, Nucl. Phys. A 541 (1992) 585.

<center>Figures captions.</center>

- Figure 1: Feynman diagram for the inelastic lepton-nucleon scattering.
- Figure 2: Lepton selfenergy diagram associated with the quasielastic lepton-nucleon scattering.
- Figure 3: Results for $\nu W_{2A}/A$ for ^{56}Fe ($Q^2 = 1.27$ GeV^2 when $x = 1$). Dot-dashed line: inelastic contribution using the nucleon structure function of [41]; dashed line: quasielastic contribution; solid line: whole calculation including the inelastic and quasielastic contributions. Experimental points from ref. [33].
- Figure 4: Same as in fig. 3 but in this case $Q^2 = 3.1$ GeV^2 when $x = 1$.
- Figure 5: Same as in fig. 3 but in this case $Q^2 = 6.83$ GeV^2 when $x = 1$ and the experimental points are from ref. [34].
- Figure 6: Results of the quasielastic channel using different approximations ($Q^2 = 1.27$ GeV^2 when $x = 1$). Solid line: spectral function; dashed line: non interacting Fermi sea, eq. (13); dot-dashed line: uncorrelated momentum distribution, eq. (14). Experimental points from ref. [33].
- Figure 7: Results of the inelastic channel using different approximations ($Q^2 = 6.83$ GeV^2 when $x = 1$). Solid lines: spectral function; dashed line: non interacting Fermi sea, eq. (13); dot-dashed line: uncorrelated momentum distribution, eq. (14). Experimental points from ref. [34].
- Figure 8: Results for the quasielastic and inelastic contributions for ^{56}Fe at $x = 1$ as a function of Q^2. Solid line: quasielastic contribution; long-dashed line: inelastic contribution using the CTEQ parametrization; short-dashed line: inelastic contribution using the MRS parametrization; dot-dashed line: inelastic contribution using the parametrization that includes the low lying resonances and a continuum part [41].
- Figure 9: Same as in fig. 8 but for $x = 0.8$.
- Figure 10: Same as in fig. 8 but for $x = 1.3$.
- Figure 11: Results for the structure function of ^{12}C at $Q^2 = 85$ GeV^2 using different parametrizations for the nucleon structure function. Solid line: MRS [49]; long-dashed line: CTEQ [50]; short-dashed line: Duke and Owens [51]. Experimental points from ref. [31].
- Figure 12: Results for $\nu W_{2A}/A$ for ^{56}Fe ($Q^2 = 1.27$ GeV^2 when $x = 1$). Dot-dashed line: inelastic contribution using the MRS parametrization of the nucleon structure function; dashed line: quasielastic contribution; solid line:whole calculation including the inelastic and quasielastic contributions. Experimental points from ref. [33].
- Figure 13: Same as in fig. 12 but in this case $Q^2 = 6.83$ GeV^2 when $x = 1$ and the experimental points are from ref. [34].
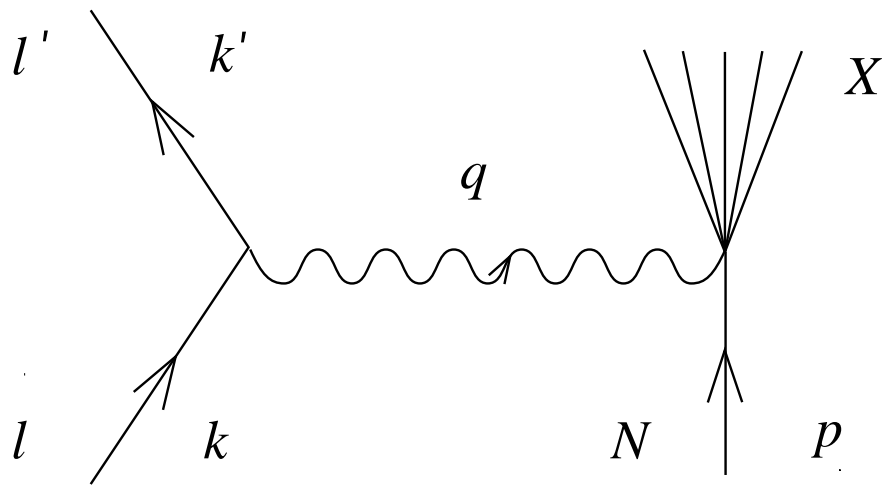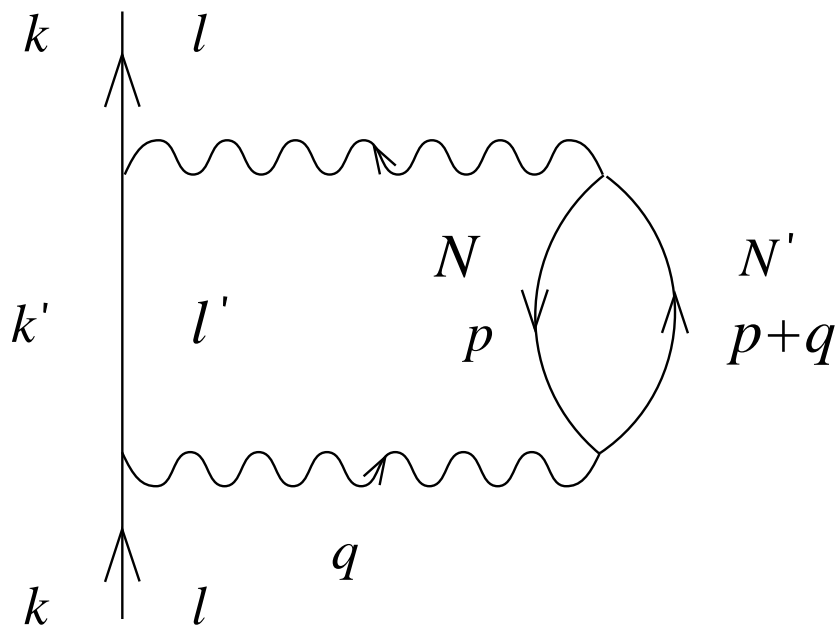
<center>17</center>

Fig. 1

Fig. 2

$\nu\, W_{2A}/A$

x

$Q^2 = 6.83$ GeV^2 (x=1)

^{56}Fe

$Q^2 = 6.83 \text{ GeV}^2 \ (x=1)$

^{56}Fe

x

$\nu W_{2A}/A$

^{56}Fe ($x=0.8$)

$^{56}Fe \; (x=1.3)$

Q^2

$\nu \, W_{2A}/A$